Department of Chemistry

Surface Functionalization by Atomic Layer Deposited Binary Oxide Thin Films

Jari Malm

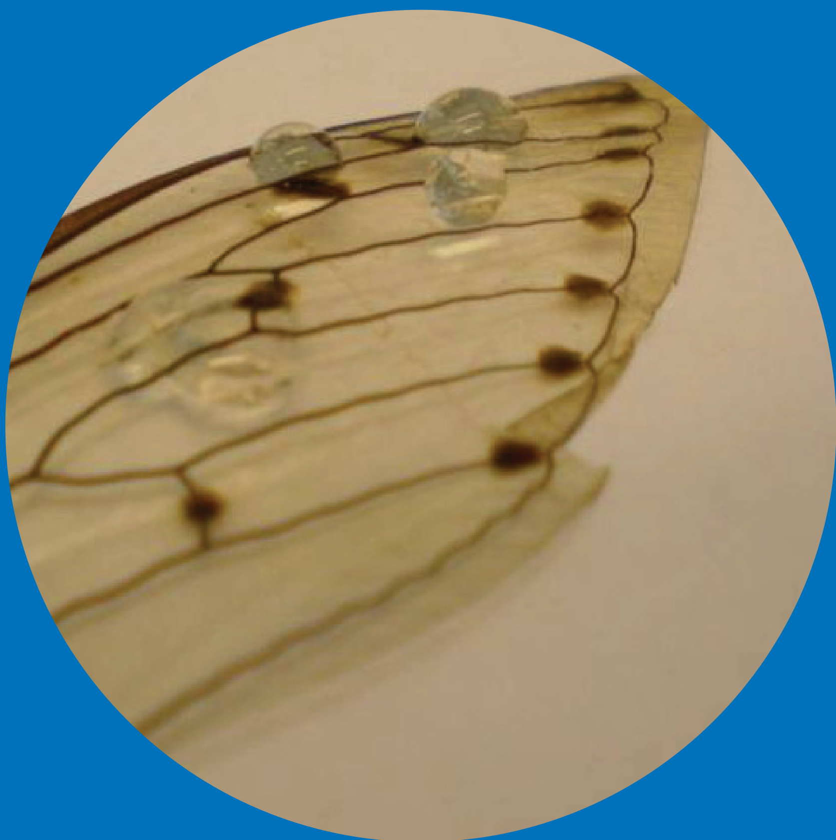

Aalto University

DOCTORAL DISSERTATIONS

Aalto University publication series
DOCTORAL DISSERTATIONS 57/2013

Surface Functionalization by Atomic Layer Deposited Binary Oxide Thin Films

Jari Malm

Doctoral dissertation for the degree of Doctor of Science in Technology to be presented with due permission of the School of Chemical Technology for public examination and debate in Auditorium KE2 (Komppa Auditorium) at the Aalto University School of Chemical Technology (Espoo, Finland) on the 3rd of May, 2013, at 12 noon.

Aalto University
School of Chemical Technology
Department of Chemistry
Laboratory of Inorganic Chemistry

Supervising professor
Academy Professor Maarit Karppinen

Preliminary examiners
Professor Jaan Aarik, University of Tartu, Estonia
Associate Professor Annelies Delabie, KU Leuven, Belgium

Opponent
Professor Kornelius Nielsch, University of Hamburg, Germany

Aalto University publication series
DOCTORAL DISSERTATIONS 57/2013

© Jari Malm

ISBN 978-952-60-5103-1 (printed)
ISBN 978-952-60-5104-8 (pdf)
ISSN-L 1799-4934
ISSN 1799-4934 (printed)
ISSN 1799-4942 (pdf)
http://urn.fi/URN:ISBN:978-952-60-5104-8

Unigrafia Oy
Helsinki 2013

Finland

441 697
Printed matter

A! Aalto University

Aalto University, P.O. Box 11000, FI-00076 Aalto www.aalto.fi

Abstract

Author
Jari Malm

Name of the doctoral dissertation
Surface Functionalization by Atomic Layer Deposited Binary Oxide Thin Films

Publisher School of Chemical Technology

Unit Department of Chemistry

Series Aalto University publication series DOCTORAL DISSERTATIONS 57/2013

Field of research Inorganic Chemistry

Manuscript submitted 14 January 2013 **Date of the defence** 3 May 2013

Permission to publish granted (date) 19 March 2013 **Language** English

☐ **Monograph** ☒ **Article dissertation (summary + original articles)**

Abstract

The materials of today have intriguing properties. The mastering of phenomena at the nanometer range often forms the basis for the understanding of novel materials and their functional properties. In this thesis three materials - zinc oxide (ZnO), titanium dioxide (TiO_2) and tungsten trioxide (WO_3) - in the form of thin films less than 100 nanometers in thickness are being studied from the surface functionalization point of view. The film application method used was atomic layer deposition (ALD).

First, the low-temperature deposition features of ZnO were studied. The deposition could be performed at as low as room temperature. Below 70 °C the hexagonal wurzite structure of ZnO oriented along the *c* axis, and above this temperature orientation along the *a* axis was also observed. The crystallinity improved in post-deposition annealings at 400–600 °C in argon and oxygen atmospheres while keeping the original preferential orientation unchanged. ZnO was also used to study the tailoring of a natural template, the wing surface of the cicada (Pomponia Intermedia) insect. The nanoscale pillar structure of the cicada wing could be area-selectively coated with a 100 nm thick ZnO film in the interstitial space between the pillars. By applying a thin aluminum oxide seed layer prior to ZnO deposition the wing nanostructure could be uniformly coated. Furthermore, the water wettability of the cicada wing was studied. The originally superhydrophobic wing surface was coated with ZnO while keeping the original superhydrophobicity almost intact. When exposed to ultraviolet (UV) light the surface was successfully turned hydrophilic and back to hydrophobic under storage in dark. The tunable wettability phenomenon was used to demonstrate directing fluid flows on planar, ZnO-coated quartz surfaces utilizing hydrophilic patterns irradiated on a hydrophobic surface by UV laser. The reversible patterning may find use in microfluidic and lab-on-a-chip devices.

TiO_2 is a common ALD film material capable of being deposited at low temperatures. Here its possibilities were demonstrated by depositing a TiO_2 layer on nanofibrillated cellulose (NFC) template, and after removal of the template using the formed TiO_2 nanotube network in a dropcast form as a humidity sensor. The usable relative humidity range was 40–80 % where the dropcast sensor layer gave repeatable resistive and capacitive response.

Finally a new ALD process of WO_3 films from $W(CO)_6$ and O_3 was introduced. The ALD temperature window was observed at 195–205 °C with a deposition rate of 0.23 nm/cycle. This process provides a straightforward option for the ALD of WO_3 as opposed to the methods based on in situ generated oxyfluoride intermediates published earlier.

Keywords Atomic layer deposition, thin film, funtionalization, wettability, ultraviolet, humidity, zinc oxide, titanium dioxide, tungsten trioxide

ISBN (printed) 978-952-60-5103-1 **ISBN (pdf)** 978-952-60-5104-8

ISSN-L 1799-4934 **ISSN (printed)** 1799-4934 **ISSN (pdf)** 1799-4942

Location of publisher Espoo **Location of printing** Helsinki **Year** 2013

Pages 78 **urn** http://urn.fi/URN:ISBN:978-952-60-5104-8

Aalto-yliopisto

Aalto-yliopisto, PL 11000, 00076 Aalto www.aalto.fi

Tiivistelmä

Tekijä
Jari Malm

Väitöskirjan nimi
Pintojen funktionalisointi atomikerroskasvatuksella valmistettujen binääristen oksidiohutkalvojen avulla

Julkaisija Kemian tekniikan korkeakoulu

Yksikkö Kemian laitos

Sarja Aalto University publication series DOCTORAL DISSERTATIONS 57/2013

Tutkimusala Epäorgaaninen kemia

Käsikirjoituksen pvm 14.01.2013 **Väitöspäivä** 03.05.2013

Julkaisuluvan myöntämispäivä 19.03.2013 **Kieli** Englanti

☐ **Monografia** ☒ **Yhdistelmäväitöskirja (yhteenveto-osa + erillisartikkelit)**

Tiivistelmä

Nykypäivän uusilla materiaaleilla on mielenkiintoisia ominaisuuksia. Perustan uusien materiaalien ja niiden ominaisuuksien ymmärtämiselle muodostaa monesti nanometrimittakaavan ilmiöiden hallinta. Tässä väitöskirjassa tutkittiin kolmea alle 100 nanometrin paksuista ohutkalvomateriaalia - Sinkkioksidia (ZnO), titaanidioksidia (TiO_2) ja volframitrioksidia (WO_3) - pinnan funktionalisoinnin näkökulmasta. Ohutkalvot valmistettiin atomikerroskasvatus (ALD) –menetelmällä.

Aluksi tutkittiin sinkkioksidin kasvatusta matalissa lämpötiloissa. Kasvatus oli mahdollista jopa huoneenlämpötilassa. Alle 70 °C:ssa ZnO:n heksagonaalinen wurziittirakenne järjestyi pinnalle *c*-akselin suunnassa ja korkeammissa lämpötiloissa havaittiin myös *a*-akselin suuntaan järjestymistä. Kalvojen kiteisyyttä parannettiin kasvatuksen jälkeen suoritetuilla lämpökäsittelyillä 400–600 °C:ssa happi- ja argonkehissä säilyttäen samalla alkuperäinen järjestyminen. ZnO:n avulla tutkittiin myös kaskas-hyönteisen (*Pomponia Intermedia*) siiven pinnan muokkaamista. Siiven pinnan pilareista muodostuva nanorakenne päällystettiin 100 nanometrin paksuisella ZnO-kerroksella valikoivasti pilareiden väliseen tilaan. Koko pinta saatiin päällystettyä tasaisesti käyttämällä ohutta alumiinioksidipohjakerrosta sinkkioksidikerroksen alla. Myös siiven pinnan kastuvuus-ominaisuuksia tutkittiin. Superhydrofobinen, vettähylkivä pinta päällystettiin sinkkioksidilla säilyttäen alkuperäinen vettähylkivyys. Pinta voitiin muuttaa hydrofiiliseksi ultravioletti(UV) –valon avulla ja palauttaa takaisin hydrofobiseksi pimeässä ympäristössä. Muunneltavaa kastuvuutta sovellettiin nestevirtojen ohjaamisessa tasaisella pinnalla valottamalla sinkkioksidipintaa UV-laserin avulla maskin läpi ja ohjaamalla vettä syntyneissä hydrofiilisissä kanavissa. Ilmiöllä on sovelluskohteita esim. mikrofluidistiikassa.

Titaanidioksidi on tunnettu ALD-kalvomateriaali jota voidaan valmistaa matalissakin lämpötiloissa. Tässä työssä sen mahdollisuuksia havainnollistettiin kasvattamalla TiO_2-kerros nanohuokoisen selluloosan päälle ja selluloosan polttamisen jälkeen käyttämällä syntynyttä, TiO_2-nanoputkimassaa kosteusanturina. Anturi antoi toistettavan resistiivisen ja kapasitiivisen vasteen 40–80 %:n suhteellisen kosteuden alueella.

Viimeiseksi esiteltiin uusi, aiemmin julkaistuja prosesseja yksinkertaisempi volframitrioksidin ALD-prosessi $W(CO)_6$ ja O_3 –lähdeaineista. ALD-ikkuna havaittiin 195–205 °C:n alueella jolloin kasvunopeus oli 0,23 nm/sykli.

Avainsanat atomikerroskasvatus, ohutkalvo, funktionalisointi, kastuvuus, ultravioletti, kosteus, sinkkioksidi, titaanidioksidi, volframitrioksidi

ISBN (painettu) 978-952-60-5103-1 **ISBN (pdf)** 978-952-60-5104-8

ISSN-L 1799-4934 **ISSN (painettu)** 1799-4934 **ISSN (pdf)** 1799-4942

Julkaisupaikka Espoo **Painopaikka** Helsinki **Vuosi** 2013

Sivumäärä 78 **urn** http://urn.fi/URN:ISBN:978-952-60-5104-8

FOREWORD

The work presented in this thesis was carried out in the Laboratory of Inorganic Chemistry at Aalto University School of Chemical Technology (Former Helsinki University of Technology, Department of Chemistry) between April 2006 and May 2012.

First I wish to thank my supervisor, academy professor Maarit Karppinen for accepting me to perform doctoral studies in the Laboratory of Inorganic Chemistry. She is especially thanked for giving me an opportunity to carry on and develop the tradition of atomic layer deposition (ALD) in our laboratory and for giving me quite much liberty in this task. Former researchers of the laboratory, Dr. Matti Putkonen, Dr. Pia Myllymäki and Ph.D. Charles Dezelah, are thanked for introducing me the practical aspects of ALD research. Special thanks also belong to Dr. Robin H. A. Ras who has been a fruitful source of ideas for our research in the beginning of this work. Ms. Elina Sahramo and Mr. Juuso Korhonen are thanked for successful co-operation over the years. Docent Timo Sajavaara from University of Jyväskylä is thanked for his expertise in performing RBS and TOF-ERDA measurements. Finally, support from the entire former and present staff and colleagues at the Laboratory of Inorganic Chemistry is greatly appreciated.

My parents Åke and Maila are warmly thanked for their care and understanding over the course of this work. I also wish to mention my former chemistry teacher at the senior secondary school Lahden Yhteiskoulu, Mrs. Anna-Liisa Harvela, who is warmly reminisced for her encouragement and support during my very first steps in the world of chemistry.

The Graduate School of Inorganic Materials Chemistry (EMTKO), the Finnish Foundation for Technology Promotion (TES), and the Emil Aaltonen Foundation are acknowledged for financial support.

Jari Malm

Espoo, January 2013

"There is progress whether ye are going forward or backward. The thing is to move."

-Edgar Cayce (1877-1945)

LIST OF CONTENTS

List of publications i
The author's contribution ii
List of abbreviations iii

1. INTRODUCTION 1
2. THE ATOMIC LAYER DEPOSITION METHOD 3
  2.1 The ALD principle 4
    2.1.1 ALD window 5
    2.1.2 Precursors 6
3. FOREWORD FOR THE EXPERIMENTS 7
  3.1 Thin film depositions 8
  3.2 UV exposure and contact angle measurements 8
  3.3 Characterization 8
4. SURFACE FUNCTIONALIZATION BY ZINC OXIDE 10
  4.1 The low temperature ALD of ZnO 10
  4.2 Area-selective ALD of ZnO 12
  4.3 Tunable wettability effect of ZnO films deposited on nanoscale structures 14
  4.4 Hydrophilic patterning of ZnO films 15
5. SURFACE FUNCTIONALIZATION BY TITANIUM DIOXIDE. 17
  5.1 Humidity sensing with TiO_2 18
6. ALD PROCESS OF TUNGSTEN TRIOXIDE 19
  6.1 Results 20
  6.2 Discussion 22
7. CONCLUSIONS 24
REFERENCES 25

LIST OF PUBLICATIONS

In addition to the present review, this thesis includes the following publications (**I–VI**), which are referred to in the text by their corresponding Roman numerals. The original publications are found in appendices **I–VI**.

I R. H. A. Ras, E. Sahramo, J. Malm, J. Raula, and M. Karppinen, Blocking the Lateral Film Growth at the Nanoscale in Area-Selective Atomic Layer Deposition, *Journal of the American Chemical Society* **130** (2008) 11252–11253.

II J. Malm, E. Sahramo, M. Karppinen, and R. H. A. Ras, Photo-Controlled Wettability Switching by Conformal Coating of Nanoscale Topographies with Ultrathin Oxide Films, *Chemistry of Materials* **22** (2010) 3349–3352.

III V. Kekkonen, A. Hakola, T. Kajava, E. Sahramo, J. Malm, M. Karppinen, and R. H. A. Ras, Self-Erasing and Rewritable Wettability Patterns on ZnO Thin Films, *Applied Physics Letters* **97** (2010) 044102-1–044102-3.

IV J. Malm, E. Sahramo, J. Perälä, T. Sajavaara, and M. Karppinen, Low-Temperature Atomic Layer Deposition of ZnO Thin Films: Control of Crystallinity and Orientation, *Thin Solid Films* **519** (2011) 5319–5322.

V J. T. Korhonen, P. Hiekkataipale, J. Malm, M. Karppinen, O. Ikkala, and R. H. A. Ras, Inorganic Hollow Nanotube Aerogels by Atomic Layer Deposition onto Native Nanocellulose Templates, *ACS Nano* **3** (2011) 1967–1974.

VI J. Malm, T. Sajavaara, and M. Karppinen, Atomic Layer Deposition of WO_3 Thin Films using $W(CO)_6$ and O_3 Precursors, *Chemical Vapor Deposition* **18** (2012) 245–248.

THE AUTHOR'S CONTRIBUTION

Publication **I** The author defined the research plan together with the co-authors and partially performed the depositions and sample characterization. The author had a minor role in writing the manuscript.

Publication **II** The author defined the research plan together with the co-authors and partially performed the depositions and sample characterization. The author had a major role in writing the manuscript.

Publication **III** The author defined the research plan together with the co-authors and performed the depositions. The author had a minor role in writing the manuscript.

Publication **IV** The author defined the research plan together with the co-authors and had a major role in performing the depositions, sample characterization and writing the manuscript.

Publication **V** The author had a supporting role in performing the depositions and in writing the manuscript.

Publication **VI** The author defined the research plan, performed the depositions and sample characterization excluding TOF-ERDA, and wrote the manuscript.

Espoo 14th of January 2013

Acad. Prof. Maarit Karppinen

LIST OF ABBREVIATIONS

AFM	Atomic force microscopy
ALD	Atomic layer deposition
ALE	Atomic layer epitaxy
CNT	Carbon nanotube
CVD	Chemical vapor deposition
DEZ	Diethyl zinc
EL	Electroluminescent
FTO	Fluorine-doped tin oxide
GPC	Growth-per-cycle
High-κ	High permittivity
MEMS	Microelectromechanical system
MFC	Microfibrillated cellulose
MLD	Molecular layer deposition
NFC	Nanofibrillated cellulose
RC	Resistor-capacitor
RTA	Rapid thermal annealing
SAM	Self-assembled monolayer
SEM	Scanning electron microscopy
TCO	Transparent conducting oxide
TFEL	Thin film electroluminescent
TMA	Trimethyl aluminum
TOF-ERDA	Time-of-flight elastic recoil detection analysis
UV	Ultraviolet
XRD	X-ray diffraction
XRF	X-ray fluorescence

1. INTRODUCTION

In the modern age, a myriad of new exciting materials have become available. These often possess previously unimaginable properties. Novelties are commonly first introduced in military, aeronautic, medical, or otherwise high-impact applications. With time, they become available for everyone. A classroom example would be teflon – a fluorinated polymer with extremely low friction coefficient that was first used for gaskets and heat-resistant layering in military hardware. Later on it was accepted more widely in industrial applications where inertness and exceptional tribological properties were looked for. Finally the non-sticking nature of teflon made it an ideal surface material for everyman's cookware. Surprisingly, teflon was initially found by accident.[1] More examples of functional materials can be found easily: titanium nitride and tungsten carbide hard coatings for cutting tools,[2] water-vapor-permeable microporous Gore-Tex layering for sportswear,[3] high-strength steels for weight reduction in automotive industry,[4] and nanopowders as carriers of medicinal agents in the human system,[5] just to name a few examples.

One approach to tailor surface properties of a bulk material is to introduce a thin film that possesses the desired properties for the surface. In some cases a stack of films may be applied to combine several functionalities. Furthermore, to find new functionalities two or more materials with their material-specific functionalities may be combined and thus a product that possesses a tailored combination of the properties of its individual constituents, or even beyond, is obtained. It is often feasible to introduce the materials in a thin film form. Thus the functionality and special properties of the thin film are combined with a low-cost, easily obtainable bulk material.

A competitive method for making thin film structures is atomic layer deposition (ALD). [6–9] It is a highly advanced, now long-endured gas-phase deposition method that yields thin films and coatings with excellent conformality, uniformity and minimal rate of defects such as microcracks or particles. While first specifically developed and used for making electroluminescent (EL) displays illustrated in Figure 1, the method has found a diversity of suitable applications over the following years. The most

notable application today is the use of ALD for depositing dielectric high-*k* gate oxide layers for computer microprocessors.[10,11]

Figure 1. The first commercial application utilizing ALD: The flight information displays by Lohja Corp. Display Electronics Division installed at Helsinki-Vantaa airport in 1983.[12]

In this thesis the ALD processes of three inorganic binary oxides - ZnO, TiO_2 and WO_3 - were investigated. These oxides are abundantly available in Earth's crust and well characterized in the bulk form, but they possess certain properties that may be utilized by applying them on the surfaces of bulk objects in the thin film form. In this thesis the ZnO, TiO_2 and WO_3 thin films were mostly studied from the surface functionalization and tailoring point of view. Surface modification experiments have been conducted with ZnO and TiO_2, whereas for WO_3 a new ALD process is presented. The potential applications of the ALD films studied are discussed.

2. THE ATOMIC LAYER DEPOSITION METHOD

Atomic layer deposition (ALD) is a gas-phase thin film deposition method often considered as a subcategory of chemical vapor deposition (CVD). However, in ALD the reactants commonly known as precursors are introduced on the substrate pulse-wise one at a time separated by inert gas purging periods contrary to CVD where the precursors are introduced simultaneously. ALD and CVD methods partially share the same precursor selection. Also other features of ALD processes can be derived or estimated from their closely resembling CVD counterparts, such as precursor evaporation and deposition temperature range, film crystallinity, and typical precursor behavior related to surface reactions, to mention some. The ALD technique has traditionally been applied for fabricating binary oxide, sulfide and nitride thin films but recently also pure metal and complex oxide films have been deposited. In case of using organic or a combination of organic and inorganic precursors the ALD method is named today as molecular layer deposition (MLD). The ALD method was originally known as atomic layer epitaxy (ALE), a term which is nowadays reserved for examples of strictly epitaxial growth only. Other names for the ALD method have been suggested, but ALD has become the generally best known one, being analogous to CVD.[6–9]

In its present form ALD has become known by the work initiated by Suntola et al. [13,14] in the 1970's. It should be noted however that ALD-like deposition of SiO_2 was reported in the Soviet Union as early as in 1966.[15] The ALE/ALD method was being developed in the first place uniquely to make electroluminescent thin film (TFEL) displays. Since the filing of the first patents it took almost a decade to mature the ALD technology enough for first commercial TFEL applications. Over the years, the method has become increasingly known and popular, as is evident in Figure 2 where the number of annually published papers and patents from 1976 till 2011 is presented. During the early steps of ALD the interest in the method from the industry was limited by the relatively low throughput in spite of the otherwise

excellent performance characteristics of ALD compared to other methods. However, more and more applications have found use of the special advantages of ALD. Today the commercially most notable application is the use of ALD for depositing dielectric high-*k* gate oxide layers for integrated circuits.[10,11] Potential applications include three-dimensional electronics, MEMS devices, nanopatterning and surface tailoring in the nanoscale, just to mention some.

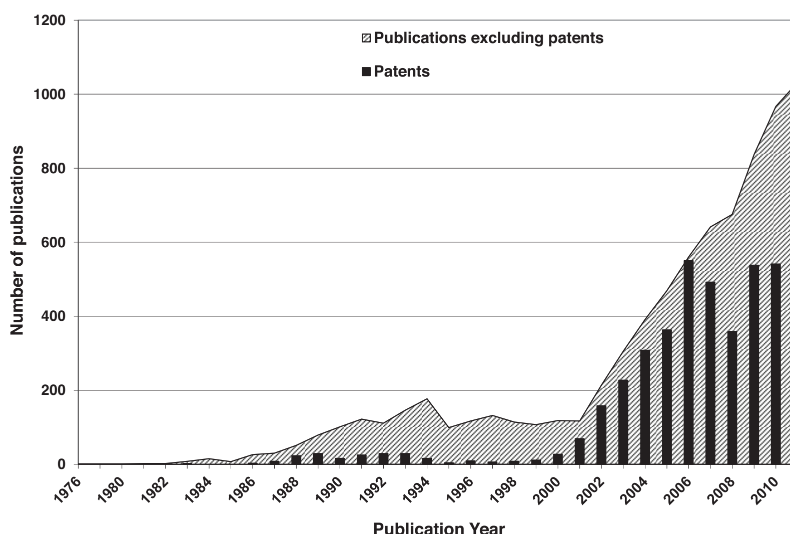

Figure 2. The number of publications and patents on ALD published annually between 1976-2011.[16]

2.1 The ALD principle

In ALD, reactive precursor vapors are introduced on a heated substrate pulse-wise keeping individual precursor vapors separated. The vapors are transported by means of an inert carrier gas (typically nitrogen). The separation of the precursors is realized by inert gas purging (in a flow-type ALD tool) or simply by long enough pumping between precursor pulses (in a diffusion-type tool), the former being the more common type both in industrial and research applications and the latter being typically used in simple in-house-made research instruments. The temperature of the substrate is selected such that the surface sites of the substrate become saturated with a monolayer of precursor molecules, while simultaneously keeping precursor pulse times long enough to allow complete surface saturation. In practice, however, the surface coverage is often 1/3 or 1/2 of a

monolayer due to steric hindrance effects caused by large, bulky precursor ligands. Precursor bonding on the substrate surface may take place by physical or chemical interactions, and the chemical reactions involved should be irreversible. After introducing the first precursor and subsequent purging, a second precursor is introduced that reacts with the previously formed monolayer of the first precursor. In consequence of the surface reaction, a monolayer of the desired thin film is obtained. The excess vapor of the second precursor together with reaction byproducts are finally purged away from the reaction chamber, completing what is known as an ALD cycle. The alternate pulsing of precursor vapors separated by inert gas purging is repeated to yield a thin film of desired thickness. Film thickness is in many cases directly or almost directly proportional to the number of ALD cycles repeated, making the thickness control very accurate.

2.1.1 ALD window

The surface-saturating nature of ALD is traditionally illustrated with the concept known as the ALD window, which depicts the temperature range in which the deposition is surface-controlled. In this range the deposition rate, or growth rate is almost independent of deposition temperature. The deposition rate is typically expressed as growth-per-cycle (GPC) - a thickness unit of growth per one ALD cycle. Figure 3 illustrates an ALD temperature window together with the non-ideal growth modes L1, L2 and H1, H2 at low and high temperatures, respectively, that take place outside this window. The ALD window concept is most successfully demonstrated in case of binary compound depositions. For ternary compounds the situation is more complicated to express. Furthermore, in MLD of organic or inorganic/organic hybrid films the precursor molecules have a tendency not only to form a surface monolayer but also to be absorbed into the film during the precursor pulse and desorb from there during the following purge period. One can easily determine that it is difficult to judge the successfulness of an ALD process based on the ALD window concept in these cases, and thus the ALD window is lately mentioned less frequently in the literature.

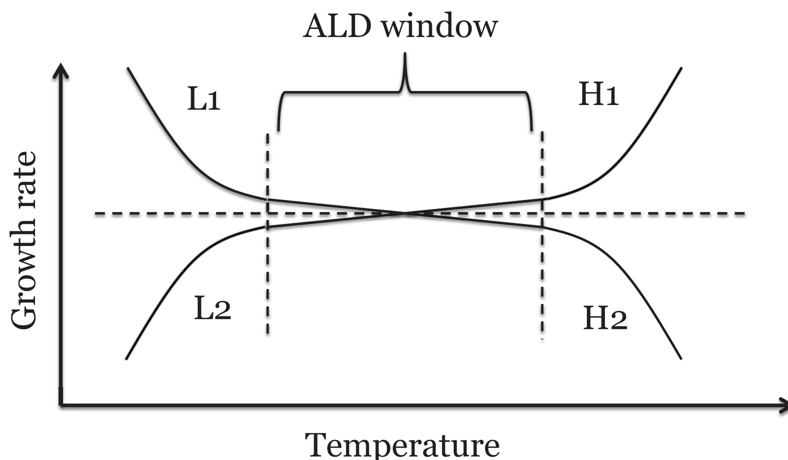

Figure 3. Illustration of the ALD window. The lines L1 and L2 represent precursor condensation and incomplete surface reaction respectively. The line H1 stands for precursor decomposition and H2 for precursor evaporation from surface due to high temperature.

2.1.2 Precursors

There are three requirements for a good ALD precursor: volatility, strong reactivity and thermal stability. Basically the precursors may be in any phase – solid, liquid or gaseous – but they should be sufficiently volatile to allow them to be carried by the carrier gas stream. The precursors may be heated to increase their vapor pressure, and different engineering techniques may be used to enhance precursor transport. In ALD the precursors should be as reactive as possible contrary to CVD where moderate reactivity is desired to prevent gas-phase reactions. Furthermore, the precursors should be thermally stable at the substrate temperature to prevent uncontrolled film deposition due to thermal precursor decomposition. Also the precursors should not dissolve in the film, and the byproducts formed from the surface reactions should be gaseous, inert and not detrimental to the ALD process. In most cases in a binary ALD process two precursors are needed; each to carry one element to the resulting ALD film. Low cost, ease of handling and non-toxicity of precursors naturally play a role in the case of industrial ALD processes.

3. FOREWORD FOR THE EXPERIMENTS

In this thesis ALD of three inorganic binary oxides, ZnO, TiO_2 and WO_3, are discussed mostly from the application point of view. In most examples presented here ALD of ZnO has been employed in various ways to tailor and functionalize surfaces. The ALD process of ZnO from diethylzinc and water has been reported previously and it is well known, but in this work special emphasis was put on low temperature depositions, even as low as room temperature. The applicability of an ALD process at this low temperature is of great importance when the depositions are performed on biological or otherwise temperature-sensitive substrates.
The ALD process for TiO_2 from titanium tetrachloride and water is also well known. TiO_2 shares many of the characteristics with ZnO. For example the tunable wettability effect upon ultraviolet illumination is found in both of these oxides. The ALD chemistries are somewhat different, but both the ALD processes are considered well understood and well-behaving.
Examples of WO_3 ALD films are much scarcer, and the previously published WO_3 processes are also rather complicated: They require the use of air-sensitive and complex precursors, or *in situ* generation of them. The main motivator for the WO_3 process was to find an easily applicable thermal WO_3 ALD process that would utilize easily attainable and operable precursors. There were no specific applications in mind for the newly developed WO_3 process, but suitable applications can be expected to be found in the smart windows or new energy technologies, especially where the conformal nature of ALD films plays a role.

A common feature for the three binary oxide materials investigated is that they are wide band-gap semiconductors with partially overlapping application areas based on their semiconducting nature: photocatalytic water splitting, self-cleaning surfaces, gas sensors, catalysts, self-cleaning surfaces, to mention some. In this thesis these materials were applied on

surfaces in thin film form and selected properties were then studied. In case of WO_3 a new ALD process was introduced, and its potential is discussed.

3.1 Thin film depositions

All of the depositions were performed in an ASM F-120 flow-type hot-wall ALD reactor in a 1-3 mbar pressure using N_2 (>99.999 %) as a carrier and purge gas generated from dry and oil-free compressed air by Schmidlin UHPN 3000-1 molecular sieve nitrogen separator. Deinoized water or ozone was used as the oxygen source. Ozone was generated from 50 l/h oxygen stream (>99.999 %) by a Fischer 502 ozone generator (estimated 5 % ozone in oxygen, corresponding to 5×10^{-5} bar ozone partial pressure under deposition conditions). Precursors for Zn, Ti, Al and W were diethylzinc (Crompton GmbH and Strem, >52 % of Zn), titanium tetrachloride (Sigma Aldrich, >99 %), trimethylaluminum (Sigma Aldrich, >97 %) and tungsten hexacarbonyl (Merck GmbH, >99.9 %), respectively.
The films were deposited on 10×5 cm^2 Si(100) and in some experiments on soda lime and quartz glass substrates. Post-deposition annealings were performed in an ATV PEO 601 rapid thermal annealing (RTA) oven in Ar and O_2 atmospheres at 600–1000 ºC.

3.2 UV exposure and contact angle measurements

For wettability experiments the UV irradiations were performed in air atmosphere in a Rayonet RPR-200 photochemical reactor equipped with 350 nm UV fluorescent tubes at ~15 cm distance from the sample. Hydrophilic patterning experiments were performed by UV irradiation though photomasks using a Lambda Physik COMPex 205 KrF excimer laser that produces 20–30 ns pulses at 248 nm wavelength. Water contact angles were measured by imaging techniques utilizing a KSV Instruments CAM 200 contact angle measurement system.

3.3 Characterization

Crystallinity and phase composition of the as-deposited and annealed films were studied by x-ray diffraction (XRD) using a Philips MPD 1880 diffractometer and Cu Kα radiation. Elemental compositions were measured using a Philips PW 1480 WDS X-ray fluorescence (XRF) spectrometer and helium atmosphere, and the data was analyzed with Uniquant 4.34 program utilizing DJ Kappa model. Surface morphology was studied by atomic force microscopy (AFM) imaging with a Ntegra PNL AFM instrument (NT-MDT Co.). Surface imaging was also performed with the

Scanning Electron Microscopy (SEM) technique using LEO DSM 982 Gemini scanning electron microscope and 2 kV acceleration voltage. The elemental compositions of ZnO and WO_3 thin films were studied with time-of-flight elastic recoil detection analysis (TOF-ERDA) technique using11.915 MeV $^{81}Br^{6+}$ and 8.515 MeV ^{35}Cl ions and 21° + 20° = 41° geometry for ZnO and WO_3 films, respectively. The thin film reflectance and transmittance spectra were recorded with a Hitachi U-2000 spectrophotometer in the 190–1100 nm wavelength range, and the reflectance spectra were used to evaluate the film thicknesses by the modeling method described by Ylilammi and Ranta-Aho.[17] In the conductivity measurements of the TiO_2 nanotube networks, the calcinated TiO_2 nanotubes were ground with ethanol as a solvent to form a slurry, which was then dropcast on fluorine tin oxide (FTO) glass substrates forming layers between 5–50 µm in thickness. The solvent was evaporated at 60 °C and the cast was subsequently calcined at 450 °C. The conductivity of the cast TiO_2 nanotube films was measured by a four-point probe setup and the samples were modeled as parallel RC circuits with Matlab and Simulink to obtain the resistance and capacitance values. Least-squares fitting of the data was performed by visually comparing the fit and the experimental data. Humidity experiments were performed in a chamber where air or argon was bubbled through deionized water. Humidity and temperature were recorded with a Vaisala HMT333 logging transmitter. Measurements were performed in the ambient temperature of 22–24 °C and the humidity was allowed to stabilize 15 minutes prior to the measurements. Furthermore, the samples were kept in dark before and during the measurements to exclude the possibility of photoinduced wetting.

4. SURFACE FUNCTIONALIZATION BY ZINC OXIDE

Most of the experiments conducted within this thesis are related to the use of zinc oxide. This binary oxide has a direct band gap of 3.3 eV and its advantageous properties include thermal and electrical stability, optical transparency, piezoelectricity, *etc.*[18] Doped ZnO has been used as a transparent conducting oxide (TCO) in solar panels and flat panel displays.[19–22] Further applications are found in gas sensors and surface tailoring with self-cleaning, non-fogging and switchable wettability characteristics.[III–IV,23–27] In some cases the preferred orientation of ZnO films plays a role in the applications.[28,29] The deposition temperature range of ZnO is relatively low as is typical for depositions from metal alkyl precursors. Low deposition temperature is an advantage when depositing on temperature-sensitive organic or biological substrates.

4.1 The low temperature ALD of ZnO

The ALD of ZnO from diethylzinc and water has been introduced in the literature several times on various substrates and at relatively low temperatures but not extending to room temperature. The ALD window region has been slightly different depending on the source as presented in Table 1.

Table 1. ALD window regions of DEZ + H_2O process presented in the literature.

ALD window region (º C)	Literature reference
room temperature	[30]
105–165	[31]
100–180	[32]
130–180	[33,34]
70–200	[35]
206–268	[36]

ALD at low temperatures typically leads to partially or completely amorphous films, depending on the film material, and in some cases, on the substrate. Not only the degree of crystallinity but also the orientation of the crystal planes may be temperature dependent. The amorphous state is preferred in barrier applications where grain boundaries of a crystallized material would serve as paths for gas diffusion which is to be avoided. In turn, the crystalline state or a specific orientation may be desirable in TCO and related applications.

The ALD of ZnO from diethylzinc and water yields slightly crystalline films of the hexagonal wurzite structure at as low as room temperature. The degree of crystallinity increases with increasing deposition temperature. Furthermore, the deposition temperature has an effect on the preferential orientation: at temperatures of up to 70 °C the films are oriented along the *c* axis, whereas films deposited at higher temperatures have a competing orientation also along the *a* axis, as presented in Figure 4. The experiments presented here do not extend beyond the 140 °C deposition temperature, but it has been reported that the orientation along the *c* axis is again increased beyond 150–200 °C deposition temperatures. [32–34]

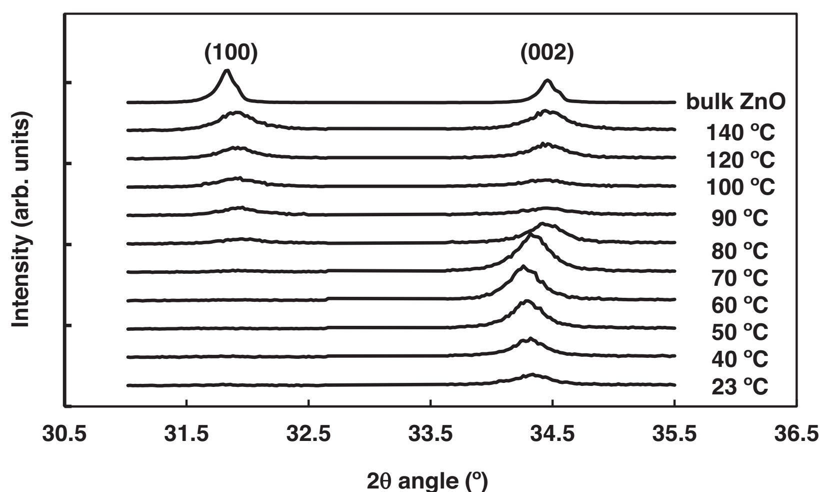

Figure 4. The development of crystallinity and preferred orientation in atomic layer deposited ZnO thin films with respect to deposition temperature.[IV]

As an interesting feature, the change in the preferential orientation is accompanied by a step-like increase in the deposition rate depicted in Figure 5. The behavior is likely to be explained by the differences in the bulk densities along the *a*- and *c*-axes of the ZnO wurtzite structure.

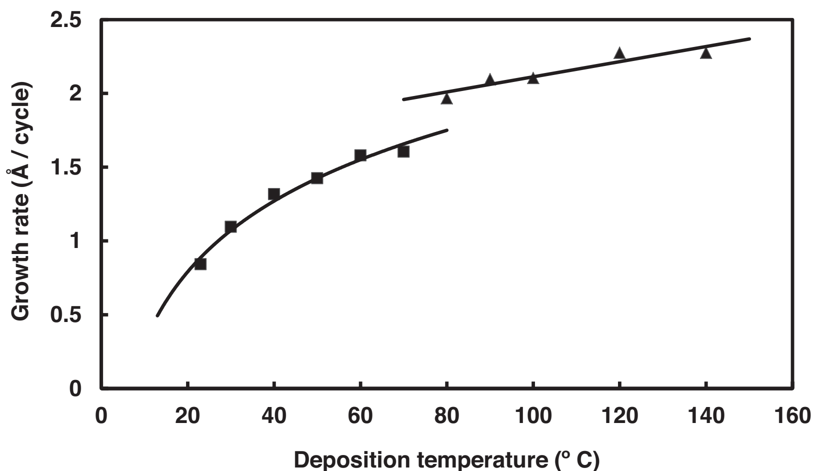

Figure 5. The step-like increase in the deposition rate of ZnO at 70–80 °C.[IV]

Crystallinity could be further improved by post-deposition annealing at 400–600 °C under oxygen or nitrogen atmospheres while keeping the originally formed preferential orientation intact. However, annealing is usually not feasible when applying ZnO films on sensitive biological substrates and furthermore, crystalline films were not specifically desired in applications presented here.

One might expect that pushing the ALD method to its limits in terms of temperature compromises film stoichiometry, homogeneity and purity, but here it was found that the low-temperature ZnO films were close to stoichiometric and hydrogen, nitrogen and carbon impurities measured with TOF-ERDA were generally low. In the temperature interval of 60–120 °C, the H and C impurities were in the range of 0.4–4.5 and 0.15–0.35 at-% respectively, and the levels of N were below 0.2 at-% throughout the range. Only in samples deposited at 40 °C the levels of H and C impurities were significantly higher, 11 and 1.1 at-% respectively.

4.2 Area-selective ALD of ZnO

Area-selectivity in ALD is typically achieved by patterning of polymer films or by the use of self-assembled monolayers (SAMs) using lithographic techniques. In these approaches means of chemistry are being utilized to leave patterned areas of the substrate surface uncovered. The use of only chemical means however has its limitations in terms of controlling the dimensions of the pattern deposited. As film thickness is increased the chemistry of the pattern is unable to efficiently define the boundaries of the

film: after a certain film thickness the film will laterally expand beyond the boundaries of the original pattern.[37]

Patterning with precisely controlled dimensions can be much more efficiently performed if the physical features of a patterned surface are combined with its chemical characteristics. Physical features may serve as effective barriers and prevent uncontrolled lateral expansion of the patterned film. Here the combination of physical and chemical means for patterning is demonstrated by using a natural template: the wing of the cicada (*Pomponia Intermedia*) insect. The cicada wing surface consists of hexagonally arranged conical nanopillars about 250 nm in height and 100 and 60 nm in diameter at the base and at the top respectively. The bulk of the wing consists mostly of crystalline chitin in a protein matrix, and the pillared wing surface is covered with a waxy layer.[38,39]

In the experiments performed with ZnO the film was deposited in the interstitial space between the cicada wing pillars, but not on the pillars themselves. When using an atomic layer deposited Al_2O_3 seed layer, however, conformal coating on the pillars was obtained, as depicted in the SEM images in Figure 6. The difference in adsorption affinity to the pillar surfaces between ZnO and Al_2O_3 may have a correlation to their crystallinity (ZnO is partly crystalline while Al_2O_3 is amorphous). The area-selectively deposited ZnO film could be peeled off from the wing substrate resulting in a free-standing nanoperforated film. ZnO layers as thick as 100 nm could be deposited in an area-selective manner while keeping the intercavity ZnO bridges of the film very narrow, approximately 25 nm matching the dimensions of the wing template. The concept of combining physical and chemical means to obtain area-selective ALD proved to be functional by using cicada wings as natural templates that were suitable for these experiments. The concept can now be extended to purposely-made templates in order to obtain desired patterning of ALD films at a very small scale.

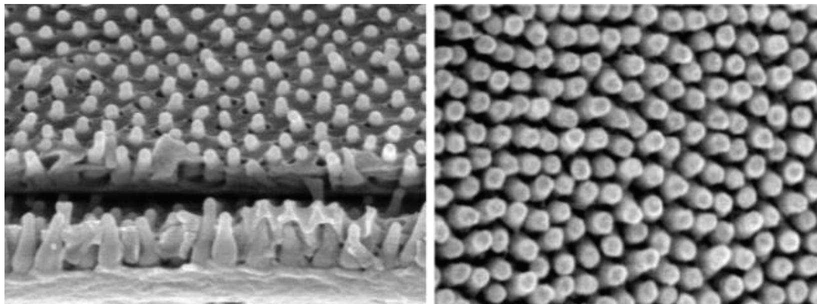

Figure 6. An area-selective deposition of ZnO on a cicada wing nanostructure (left) and the same structure conformally coated by applying an Al_2O_3 seed layer prior to ZnO deposition (right).

4.3 Tunable wettability effect of ZnO films deposited on nanoscale structures

Parts of plant and insect bodies have properties developed over millions of years of evolution. One notable property is the water wettability of these natural surfaces, where either highly hydrophilic or hydrophobic function is desirable. Surfaces having a water contact angle of over 150° are known as superhydrophobic, whereas those with contact angles lower than 5° are called superhydrophilic. The wings of the cicada insect used as templates in the experiments of this work are superhydrophobic due to their surface nanostructure and roughness. The hydrophobicity of the nanostructure is further enhanced with a water-repellent waxy layer. Thus the hydrophobic property of the cicada wing is a combination of physical and chemical factors.

The wettability of a surface can be made switchable by applying a material that changes its wettability behavior by an external stimulus, such as light, heat or electric field.[40] Binary semiconducting oxides ZnO, TiO_2, WO_3, V_2O_5 and SnO_2, for example, change their wettability from hydrophobic to hydrophilic under exposure to ultraviolet (UV) light.[41] Under storage in dark the materials return to their original hydrophobic state. The UV-induced reversible hydrophobicity is explained by photogenerated electron-hole pairs on the surface. The adsorption of the hydroxyl groups of water on the photogenerated defect sites is preferred over atmospheric oxygen absorption, which leads to hydrophilic behavior. In dark the defects are recovered, the hydroxyl groups are replaced with oxygen and the surface returns to its hydrophobic state.[42]

Here the feasibility of combining the natively superhydrophobic surface with a tunable hydrophobic/hydrophilic ZnO layer was studied.[II] Twenty cycles of Al_2O_3 from TMA and water was first applied as a seed layer to

obtain uniform ZnO coverage. ZnO films deposited by applying 10, 20, 30, 50 and 100 cycles were used to observe the wettability effect. Samples with 10 cycles of ZnO did not show any wettability change when exposed to UV light, and the maximum effect was observed with 50 and 100 cycles, 20 and 30 cycles being intermediate. Contact angle values with respect to the number of ZnO deposition cycles are presented in Figure 7. The maximum initial water contact angle was 160° on a noncoated wing and 132° on a wing coated with 100 cycles of ZnO. The difference can be explained by a minor change in the topography of the wing surface with a ZnO film on it, lowering the contact angle. The contact angle of the 100-cycle film decreased to 14° in a 10-min-long exposure to UV light and it recovered to 100° within one hour in dark. In XRF measurements an incubation period of approximately 20–50 ZnO deposition cycles was observed, where the deposition is slower than during subsequent cycles. During this period the growth is likely island-like[43] and the tunable wettability phenomenon is thus not fully effective.

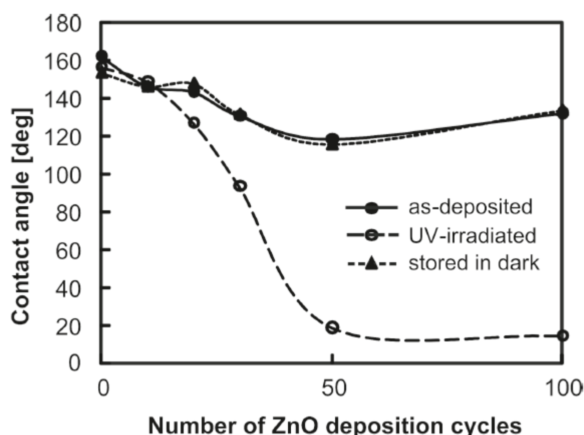

Figure 7. The effect of film thickness and UV exposure on the water contact angle of a ZnO film.[II]

4.4 Hydrophilic patterning of ZnO films

The UV tunable behavior of ZnO may be utilized in microfluidic and lab-on-a-chip devices by making hydrophilic patterns on a hydrophobic surface and thus make fluid channels without using capillaries or other physical barriers for controlling fluid flows.[44–47] In this work UV excimer laser and photomasks were used to create hydrophilic passages on a hydrophobic 100 nm thick ZnO film on quartz glass.[III] An irradiation time of 5 and 10 min decreased the contact angle from around 100° to 30° and <20°

respectively. The use of centrifugal and capillary forces was applied to encourage fluid flow, as illustrated in Figure 8. A capillary arrangement was constructed from two glass slides with a laser-irradiated hydrophilic line on them, separated by a 200 μm spacer. A 12 mm column of water could be observed in the capillary gap. A centrifugal arrangement in turn was set up by placing hydrophilically patterned glass slides on a rotating tray. With properly adjusting the speed of rotation water droplets placed on patterned areas of the glass could be moved along the hydrophilic pattern while keeping droplets placed on unpatterned areas stationary. It is noteworthy that the UV laser induced patterns are removable either spontaneously or under vacuum conditions: an 18 hour storage in vacuum completely removes the patterns and returns the contact angle completely to 99°, while an equally long storage in ambient conditions leads to a relatively high contact angle of 80°.

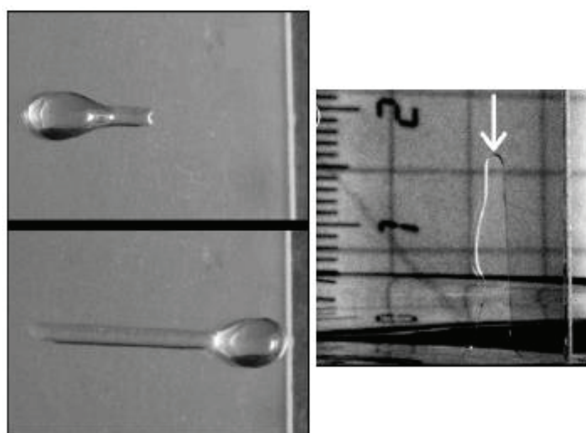

Figure 8. Transport of a water droplet along a patterned hydrophilic path aided by centrifugal force (left upper and lower) and by capillary force (right).[III]

5. SURFACE FUNCTIONALIZATION BY TITANIUM DIOXIDE

Titanium dioxide TiO_2 is an abundant material which is found in three common naturally occurring forms: Tetragonal rutile and anatase, and orthorhombic brookite. The trivial name titania typically refers to rutile which is the only thermodynamically stable phase. TiO_2 is chemically inert and insoluble, it has an extraordinarily high refractive index between 2.6–2.9 and it is an efficient UV absorbent. Thus it is widely used as a bright white pigment in paints and coatings, paper and sunscreens. Due to its nontoxicity it may even be added in foodstuffs and pharmaceuticals.

TiO_2 is not particularly known as an ALD coating to be deposited at low temperatures, contrary to the more common examples for low-temperature depositions of Al_2O_3 and ZnO from metal alkyl precursors and water. The ALD growth of TiO_2 has been demonstrated at as low as room temperature by applying special techniques,[48] but typically deposition has been carried out at 100–150 °C at lowest, which is low enough to allow deposition on many temperature-sensitive surfaces.[49–54] However, several features of the TiO_2 film are affected by deposition temperature, including crystallinity and phase composition, chlorine content, deposition rate, and uniformity. Low-temperature depositions typically lead to amorphous TiO_2 films. The etching effect from the HCl byproduct from the surface reaction should be taken into account since it may be damaging for the TiO_2 thin film and also for the underlying substrate.

In this work, the usability of atomic layer deposited TiO_2 - together with Al_2O_3 and ZnO - thin films for sensitive substrates was demonstrated by depositing them at 150 °C on nanofibrillated cellulose (NFC) aerogel template, also known as microfibrillated cellulose (MFC) or briefly nanocellulose.[V] The removal of the nanocellulose template by calcination at 450 °C led alternatively to hollow, tubular inorganic aerogel structures instead of organic-inorganic hybrid structures. In the as-deposited state some roughness of ZnO films was observed while TiO_2 and Al_2O_3 films were smooth. This is consistent with the expected crystallinity of the films: ZnO

ALD films are crystalline even at deposition temperatures well below 100 °C while TiO_2 and Al_2O_3 remain amorphous at the deposition temperature of 150 °C.

5.1 Humidity sensing with TiO_2

A bulk amount of nanotubes can be used as an additive to enhance various material characteristics. So far this has been done to a larger extent using carbon nanotubes (CNTs) for different purposes, typically for materials of construction and for polymers. Alternatively, nanotubes can be used as such to find and utilize their new functionalities. Here the humidity sensing capabilities of a film prepared from ground TiO_2 nanotube slurry were demonstrated. After removing the nanocellulose substrate by burning at 450 °C, the hollow TiO_2 nanotubes were ground with ethanol as a solvent to form a slurry, which was then dropcast on fluorine tin oxide (FTO) glass substrates forming layers between 5–50 µm in thickness, followed by drying and calcination. Conductivities of the cast films were measured with the method described in chapter 3.3. Both the resistance and capacitance of the cast TiO_2 film responded to changes in relative humidity in the range of 40–80 %, and the change observed was reversible and reproducible, as presented in Figure 9. It was suggested that the resistance response simply originates from water adsorbing on the large surface area of the nanotubes, thus increasing the conductivity of the system. The response time observed was 2 s, which is 1–2 orders of magnitude faster than response times for TiO_2 nanotube sensors reported elsewhere,[55] and as such competitive with the performance of commercial humidity sensors.

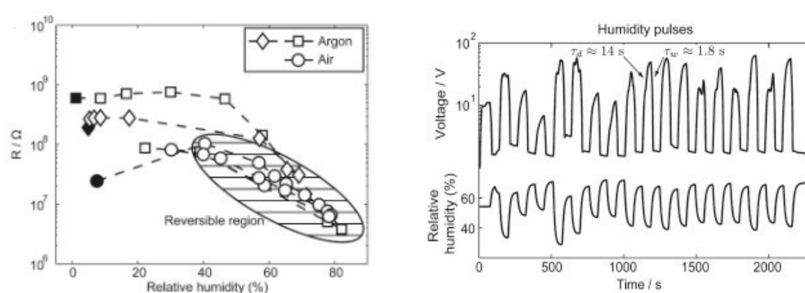

Figure 9. TiO_2 dropcast film as a humidity sensor. The resistivity response to humidity (left): Filled symbols present the start of the measurement, open squares/rhombs and open circles present measurenments under argon and air respectively. The speed and repeatability of voltage response (right).[V]

6. ALD PROCESS OF TUNGSTEN TRIOXIDE

Thin films of tungsten trioxide WO_3 and its oxygen-deficient forms WO_{3-x} possess useful properties in applications such as electrochromic[56–59], catalytic[60–67] and gas sensing devices[68–70]. Probably the best-known applications are found in electrochromic devices, one example being the automatically dimming rearview mirrors in automotive use. In recent years increasing interest has arisen in new energy technologies where the generation of hydrogen through photocatalytic decomposition of water is studied, a WO_3 film acting as a catalyst in the process.[60]

Enhanced performance is commonly achieved for WO_3 in its applications by doping, by combining it with other metal oxides, and by using tailored geometries or nanostructures. Several well-known CVD and physical vapor deposition (PVD) processes exist for fabricating tungsten oxide thin films.[71]

Not many ALD processes for tungsten oxides have been published before. Atomic layer deposited WO_3 films have previously been deposited from WF_6 and *in-situ* generated hexavalent tungsten oxyfluoride[72], and from a $(t\text{BuN})_2(\text{Me}_2\text{N})_2\text{W}$ amide precursor.[60] W_2O_3 films with trivalent tungsten have been deposited from the air-sensitive $W_2(NMe_2)_6$ precursor and H_2O by ALD.[73] In the present thesis the atomic layer deposition of WO_3 thin films on Si(100) substrates is presented. $W(CO)_6$ as the tungsten source and O_3 as the secondary reactant and as the oxygen source to decompose $W(CO)_6$ yielding WO_3 thin films is presented for the first time. The use of carbonyl precursors in ALD has been reported only a few times.[74–76] Among these, only one process is utilizing a homoleptic carbonyl precursor in thermal ALD – the MoO_3 process from $Mo(CO)_6$ andO_3/H_2O mixture.[77] One MLD process utilizing $V(CO)_6$ and tetracyanoethylene has also been published recently.[78]

6.1 Results

Preliminary WO_3 deposition experiments were carried out in the temperature range of 150 – 400 °C and visually acceptable and uniform growth was achieved at 160–225 °C. At temperatures lower than this the growth rate was extremely slow whereas at higher temperatures the films appeared non-uniform and dark, indicating thermal decomposition of the carbonyl precursor. In addition to the deposition temperature, the process was also sensitive to the precursor evaporation temperature. Too low or high evaporation temperatures were found to result in growth rate variations and uneven growth. Due to the design of the F-120 ALD reactor, temperature control of solid precursors at low temperatures is demanding to keep consistent. The $W(CO)_6$ precursor boat was situated inside the reactor at as cool location as possible at the very end of a precursor tube, essentially at room temperature. Some heat is radiated to this location from the heated sections of the reactor, however.

$W(CO)_6$ pulse lengths of 1–5 s were studied. Within this time frame the $W(CO)_6$ pulse length had some effect on the growth rate, thus in spite of good overall control over the deposition there was a minor CVD component involved. While all pulse lengths gave relatively uniform deposition, 3 s was the shortest time to yield uniform films throughout the entire deposition area. Thus 3-s-long $W(CO)_6$ pulses were used together with 2-s-long O_3 pulses and 5-s-long N_2 purges. The growth rate was almost linear in the temperature range of 160–225 °C but a narrow ALD temperature window was found between 195–205 °C with a growth rate of 0.23 nm/cycle as illustrated in Figure 10. The WO_3 deposition from oxyfluorides, in turn, has a lower growth rate of 0.08 nm/cycle at a single temperature of 200 °C studied.[72]

The closely-resembling MoO_3 process also has a lower growth rate of 0.07 nm/cycle in an ALD window between 157–172 °C when ozone alone or combined with water is used as an oxygen source. Using water only gives even lower deposition rates for MoO_3.[77]

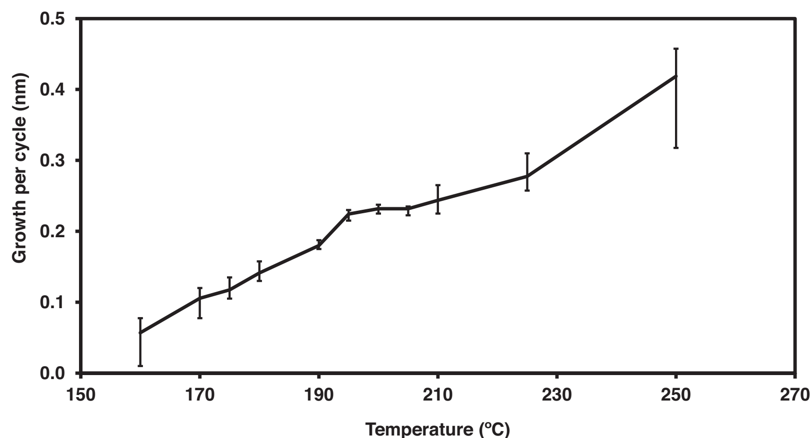

Figure 10. WO_3 deposition rate as a function of temperature. Growth rate variation within sample area is illustrated by vertical bars.[VI]

As-deposited WO_3 films were smooth as observed by AFM. A granular texture started to develop in thermal annealing, higher annealing temperatures giving more granular or more crystalline surface appearance. Annealing at the highest temperature of 1000 °C developed microcracks and a visually dull, foggy appearance on the films. Annealing atmosphere had an influence on the granularity, samples annealed under oxygen being more granular than those annealed under nitrogen. Not only granularity but also crystallinity improved under annealings, which was clearly seen as increasing peak intensities in XRD data. The correlation between crystallinity and surface morphology may be observed below in XRD patterns and AFM images in Figure 11 and Figure 12, respectively. The morphology is considerably different from MoO_3 films by Diskus *et al.*[77] especially with respect to uniformity: WO_3 films give full surface coverage whereas MoO_3 tends to deposit in an island-like manner.

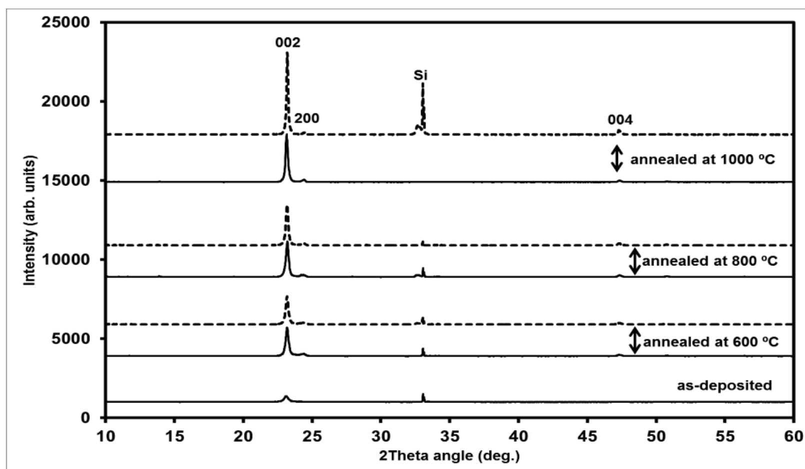

Figure 11. XRD patterns of WO_3 films as-deposited at 200 °C and annealed at 600–1000 °C under N_2 (solid lines) and O_2 (dashed lines) atmospheres. The indices are for triclinic WO_3 phase.[VI]

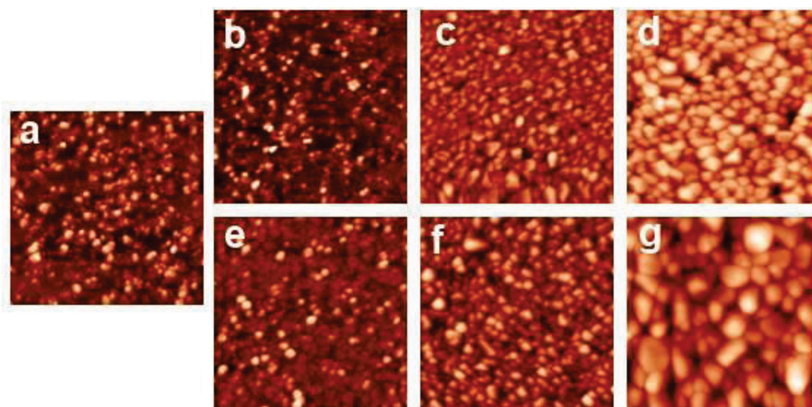

Figure 12. AFM images of as-deposited and annealed WO_3 film surfaces: (a) As-deposited, and annealed at (b) 600, (c) 800 and (d) 1000 °C in N_2 and in O_2 (e, f, g) atmospheres, respectively.[VI]

The RMS roughness values increased upon annealings and varied between 4.7–16.4 nm in a 2 × 2 µm area. WO_3 films were stoichiometric and had negligible carbon and nitrogen impurities, generally below 0.1 at-%.

6.2 Discussion

The ALD window found in the present work for the $W(CO)_6$ / O_3 ALD process was relatively narrow, between 195–205 °C which is expected for processes utilizing precursors with weak precursor-surface interactions. Another indication of the low reactivity is the sensitivity of the process (in

terms of deposition rate and uniformity) to other factors than the deposition temperature, such as precursor evaporation temperature, and also to some extent, precursor pulse length. It should be noted however that the alternative WO_3 deposition approach utilizing oxyfluoride intermediates also suffers from sensitivity to variations in process conditions related to the generation of the oxyfluoride species, and that the presence of fluorine leaves about 2 at-% of fluorine impurity in the films.[72] The straightforward utilization and precursor chemistry together with a relatively high deposition rate and low impurity levels makes the utilization of $W(CO)_6$ competitive compared to the use of *in situ* generated oxyfluorides demonstrated earlier. It also adds a new member to the selection of so far very few carbonyl precursors used in ALD.

7. CONCLUSIONS

In this work three ALD materials – ZnO, TiO_2 and WO_3 – were studied. ZnO was studied the most thoroughly from the viewpoint of its applicability to low temperature depositions and various surface tailoring applications. ZnO is especially suitable when crystalline films are to be deposited at low temperatures, since its common competitor Al_2O_3 gives completely amorphous ALD films and needs an annealing temperature of over 900 ºC to crystallize, making impossible to obtain crystalline Al_2O_3 on sensitive substrates. ZnO is shown to give conformal films on large aspect ratio biological structures in the nanoscale i.e. on cicada wing surfaces, for example. Interestingly it was found that the chemistry on a cicada wing together with the topography is influencing the deposition leading to area-selective ALD growth, and a ZnO film with a perforated pattern is obtained. Conformality is only obtained by using an Al_2O_3 seed layer prior to ZnO deposition. The UV switchable wettability property of ZnO was utilized to demonstrate that the wettability of a natively superhydrophobic cicada wing can be reversibly altered to hydrophilic under UV light by applying a thin ZnO film on the wing nanostructure. Control of fluid flow by using UV-laser-irradiated hydrophilic patterns on a planar hydrophobic ZnO film surface was also demonstrated.

TiO_2 as well as ZnO may be deposited at low temperatures by ALD, thus allowing them to be applied on temperature sensitive surfaces. A dropcast layer of inorganic nanotubes prepared by ALD of TiO_2 on a nanocellulose network could be used as a humidity sensor comparable in performance to those of commercial origin in the relative humidity range of 40–80 %. The resistivity and capacitance changes of the TiO_2 film are explained by water adsorption on the large surface area of the dropcast nanotube layer, increasing its conductivity.

For WO_3 a new ALD process from $W(CO)_6$ and O_3 was introduced with an ALD window between 195–205 ºC. This straightforward thermal ALD process utilizing relatively nontoxic and stable precursors provides a facile way to deposit good quality WO_3 films with minimal impurities.

REFERENCES

[1] PPS Technology, The History of PTFE, *http://www.ppstechnology.com/Assets/PDF/PTFEHistory.pdf*, 24 October 2012.

[2] G. M. Demyashev, A. L. Taube, E. Siores, Superhard nanocomposites. In *Encyclopedia of Nanoscience and Nanotechnology*, Vol. **10**, pp. 191–236, Ed. H. S. Nalwa, American Scientific Publishers, Stevenson Ranch, CA, USA, 2004.

[3] R. R. Mather, *Rev. Prog. Color. Relat. Top.* **31** (2001) 36.

[4] H. Hofmann, D. Mattissen, T. W. Schaumann, *Steel Res. Int.* **80** (2009) 22.

[5] R. Mout, D. F. Moyano, S. Rana, V. M. Rotello, *Chem. Soc. Rev.* **41** (2012) 2539.

[6] V. Miikkulainen, M. Leskelä, M. Ritala, R. L. Puurunen, *J. Appl. Phys.* **113** (2013) 021301.

[7] S. George*, Chem. Rev.* **110** (2010) 111.

[8] M. Ritala, J. Niinistö, Atomic Layer Deposition, in *Chemical Vapour Deposition* (eds. A. C. Jones, M. L. Hitchman), Royal Society of Chemistry, Cambridge, UK **2009,** p. 158.

[9] M. Leskelä, M. Ritala, Atomic Layer Deposition. In *Handbook of Thin Film Materials*, Vol **1**, Ed. H. S. Nalwa, Academic Press, San diego 2001, 103p.

[10] J. A. Kittl, K. Opsomer, M. Popovici, N. Menou, B. Kaczer, X. P. Wang, C. Adelmann, M. A. Pawlak, K. Tomida, A. Rotschild, B. Govoreanu, R. Degraeve, M. Schaekers, M. Zahid, A. Delabie, J. Meersschaut, W. Polspoel, S. Clima, G. Pourtois, W. Knaepen, C. Detavernier, V. V. Afanas'ev, T. Blomberg, D. Pierreux, J. Swerts, P. Fischer, J. W. Maes, D. Manger, W. Vandervorst, T. Conard, A. Franquet, P. Favia, H. Bender, B. Brijs, S. Van Elshocht, M. Jurczak, J. Van Houdt, D. J. Wouters, *Microelectron. Eng.* **86** (2009) 1789.

[11] J. Niinistö, K. Kukli, M. Heikkilä, M. Ritala, M. Leskelä, *Adv. Eng. Mater.* **11** (2009) 223.

[12] Finnish Industrial Design Archives, Jukka Vaajakallio's collection, *http://www.elka.fi/fida/index.php?id=69&page=Vaajakallio%20Design%20Oy*, 15 October 2012.

[13] T. Suntola, J. Antson, *U. S. Patent* No. 4 058 430 (1977).

[14] T. Suntola, *Mater. Sci. Rep.* **4** (1989) 261.

[15] A. M. Shevyakov, G. N. Kuznetsova, V. B. Aleskovskii*, Khim. Vysokotemp. Mater., Tr. Vses. Soveshch.* **2** (1965) 149.

[16] *The American Chemical Society, Chemical Abstract Service*, keywords: Atomic layer deposition OR atomic layer epitaxy, 24 October 2012.

[17] M. Ylilammi, T. Ranta-Aho, *Thin Solid Films* **232** (1993) 56.

[18] Ü. Özgür, Ya. I. Alivov, C. Liu, A. Teke, M.A. Reshchikov, S. Doğan, V. Avrutin, S.-J. Cho, H. Morkoç, *J. Appl. Phys.* **98** (2005) 041301.

[19] J.-H. Lee, B.-O. Park, *Thin Solid Films* **426** (2003) 94.

[20] M. Ohyama, H. Kozuka, T. Yoko*, J. Am. Ceram. Soc.* **81** (1998) 1622.

[21] T. Minami, H. Kumagai, T. Kakumu, S. Takata, M. Ishii, *J. Vac. Sci. Technol. A* **15** (1997) 1069.

[22] H. Sato, T. Minami, S. Takata, T. Mouri, N. Ogawa, *Thin Solid Films* **220** (1992) 327.

[23] F. Gladis, A. Eggert, R. Schumann “by” F. Gladis, A. Eggert, U. Karsten, R. Schumann, *Biofouling* **26** (2010) 89.

[24] S. Patra, S. Sarkar, S.K. Bera, R. Ghosh, G.K. Paul, *J. Phys. D Appl. Phys.* **42** (2009) 075301.

[25] S. Kathirvelu, L. D'Souza, B. Dhurai, *Indian J. Sci. Technol.* **1** (7) (2008), 12 pages.

[26] J. Joo, D. Lee, M. Yoo, S. Jeon, *Sens. Actuators B* **138** (2009) 485.

[27] A. Niemann, C. Schmoranzer, R. Grunwald, W. Seeber, *Phys. Chem. Glasses* **49**

(2008) 55.

[28] J.-H. Lee, B.-O. Park, *Thin Solid Films* **426** (2003) 94.

[29] M. Ohyama, H. Kozuka, T. Yoko, *J. Am. Ceram. Soc.* **81** (1998) 1622.

[30] C.-S. Ku, H.-Y. Lee, J.-M. Huang, C.-M. Lin, *Mater. Chem. Phys.* **120** (2010) 236.

[31] B. Sang, M. Konagai, *Jpn. J. Appl. Phys.* **35** (1996) L602.

[32] E. Guziewicz, I.A. Kowalik, M. Godlewski, K. Kopalko, V. Osinniy, A. Wójcik, S. Yatsunenko, E. Łusakowska, W. Paszkowicz, M. Guziewicz, M., *J. Appl. Phys.* **103** (2008) 033515.

[33] E.B. Yousfi, J. Fouache, D. Lincot, *Appl. Surf. Sci.* **153** (2000) 223.

[34] J. Lim, C. Lee, *Thin Solid Films* **515** (2007) 3335.

[35] S. Jeon, S. Bang, S. Lee, S. Kwon, W. Jeong, H. Jeon, H.J. Chang, H-H. Park, *J. Electrochem. Soc.* **155** (2008) H738.

[36] K. Saito, Y. Yamamoto, A. Matsuda, S. Izumi, T. Uchino, K. Ishida, K. Takahashi, *Phys. Status Solidi B* **229** (2002) 925.

[37] C. Bae, H. J. Shin, J. Moon, M. M. Sung, *Chem. Mater.* **18** (2006) 1085.

[38] J. F. V. Vincent, U. G. K. Wegst, *Arthropod Struct. Dev.* **33** (2004) 187.

[39] P. Kreuz, W. Arnold, A. B. Kesel, *Ann. Biomed. Eng.* **29** (2001) 1054.

[40] F. Xia, Y. Zhu, L. Feng, L. Jiang, *Soft Matter* **5** (2009) 275.

[41] X. Feng, L. Feng, M. Jin, J. Zhai, L. Jiang, D. Zhu, *J. Am. Chem. Soc.* **126** (2004) 62.

[42] R. D. Sun, A. Nakajima, A. Fujishima, T. Watanabe, K. Hashimoto, *J. Phys. Chem. B* **105** (2001) 1984.

[43] H. Makino, S. Kishimoto, T. Yamada, A. Mijake, N. Yamamoto, T. Yamamoto, *Phys. Status Solidi A* **8** (2008) 1971.

[44] X.-T. Zhang, O. Sato, A. Fujishima, *Langmuir* **20** (2004) 6065.

[45] H. Gau, S. Herminghaus, P. Lenz, R. Lipowsky, *Science* **283** (1999) 46.

[46] A. C. Muir, S. Mailis, R. W. Eason, *J. Appl. Phys.* **101** (2007) 104916.

[47] H. Nagai, T. Irie, J. Takahashi, S. Wakida, *Biosens. Bioelectron.* **22** (2007) 1968.

[48] T. Kawai, T. Choda, S. Kawai, *Mater. Res. Soc. Symp. Proc.* **75** (1987) 289.

[49] M. Ritala, M. Leskelä, E. Nykänen, P. Soininen, L. Niinistö, *Thin solid Films* **225** (1993) 288.

[50] J. Aarik, A. Aidla, A.-A. Kiisler, T. Uustare, V. Sammelselg, *Thin Solid Films* **305** (1997) 270.

[51] V. Sammelselg, A. Rosental, A. Tarre, L. Niinistö, K. Heiskanen, K. Ilmonen, L.-S. Johansson, T. Uustare, *Appl. Surf. Sci.* **134** (1998) 78.

[52] J. Aarik, A. Aidla, H. Mändar, V. Sammelselg, *J. Cryst. Growth* **220** (2000) 531.

[53] J. Aarik, A. Aidla, H. Mändar, T. Uustare, *Appl. Surf. Sci.* **172** (2001) 148.

[54] C. J. Summers, D. P. Gaillot, M. Crne, J. Blair, J. O. Park, M. Srinivasarao, O. Deparis, V. Welch, J.-P. Vigneron, *J. Nonlinear Opt. Phys. Mater.* **19** (2010) 489.

[55] Y. Zhang, W. Fu, H. Yang, Q. Qi, Y. Zeng, T. Zhang, R. Ge, G. Zou, *Appl. Surf. Sci.* **254** (2008) 5545.

[56] C. G. Granqvist, S. Green, G. A. Niklasson, N. R. Mlyuka, S. von Kræmer, P. Georén, *Thin Solid Films* **518** (2010) 3046.

[57] S. K. Deb, *Sol. Energ. Mat. Sol. Cells* **92** (2008) 245.

[58] A. Georg, A. Georg, W. Graf, V. Wittwer, *Vacuum* **82** (2008) 730.

[59] G. A. Niklasson, C. G. Granqvist, *J. Mater. Chem.* **17** (2007) 127.

[60] R. Liu, Y. Lin, L.-Y. Chou, S. W. Sheehan, W. He, F. Zhang, H. J. M. Hou, D. Wang, *Angew. Chem. Int. Ed.* **50** (2011) 499.

[61] J. Georgieva, S. Sotiropoulos, S. Armyanov, E. Valova, I. Poulios, N. Philippidis, (Ed. V. G. Singh), *Applied electrochemistry* (2010) 301.

[62] J. R. Ferrell (III), A. M. Herring, *ACS Symp. Ser.* **1040** (2010) 153.

[63] J. A. Rodriguez, D. Stacchiola, *Phys. Chem. Chem. Phys.* **12** (2010) 9557.

[64] M. M. Natile, A. Glisenti, (Eds. V. Cabral, R. Silva), *Nanomaterials* (2010) 211.

[65] L. Rizzo, (Ed. G. K. Castello), *Handbook of Photocatalysts* (2010) 271.

[66] H. Zhang, G. Chen, D. W. Bahnemann, *J. Mater. Chem.* **19** (2009) 5089.

[67] C. M. Carotta, A. Giberti, V. Guidi, C. Malagu, B. Vendemiati, G. Martinelli, *Mat. Res. Soc. Symp. Proc.* **828** (2005) 173.

[68] A. Gurlo, *Nanoscale* **3** (2011) 154.

[69] P. Heszler, R. Ionescu, E. Llobet, L. F. Reyes, J. M. Smulko, L. B. Kish, C. G. Granqvist, *Phys. Status Solidi B* **244** (2007) 4331.

[70] K. Zakrzewska, *Thin Solid Films* **391** (2001) 229.

[71] M. Jayachandran, R. Vijayalakshmi, V. Ravindran, C. Sanjeeviraja, *Trans. SAEST* **40** (2005) 42.

[72] P. Tägtström, P. Mårtensson, U. Jansson, J.-O. Carlsson, *J. Electrochem. Soc.* **146** (1999) 3139.

[73] C. L. Dezelah, O. M. El-Kadri, I. M. Szilágyi, J. M. Campbell, K. Arstila, L. Niinistö, C. H. Winter, *J. Am. Chem. Soc.* **128** (2006) 9638.

[74] V. Y. Vasilyev, *Russian Microelectron.* **39** (2010) 262.

[75] K. Lee, K. Kim, W. Jeong, T. Park, H. Jeon, *Diffus. De. B* **124–126** (2007) 359.

[76] K. Kim, K. Lee, S. Han, T. Park, Y. Lee, J. Kim, S. Yeom, H. Jeon, *Jpn. J. Appl. Phys 2* **46** (2007) L173.

[77] M. Diskus, O. Nilsen, H. Fjellvåg, *J. Mater. Chem.* **21** (2011) 705.

[78] C.-Y. Kao, J.-W. Yoo, Y. Min, A. J. Epstein, *ACS Appl. Mater. Interfaces* **4** (2012) 137.

Aalto-DD 57/2013

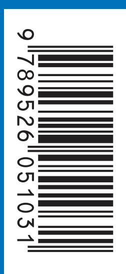

ISBN 978-952-60-5103-1
ISBN 978-952-60-5104-8 (pdf)
ISSN-L 1799-4934
ISSN 1799-4934
ISSN 1799-4942 (pdf)

Aalto University
School of Chemical Technology
Department of Chemistry
www.aalto.fi

BUSINESS +
ECONOMY

ART +
DESIGN +
ARCHITECTURE

SCIENCE +
TECHNOLOGY

CROSSOVER

DOCTORAL
DISSERTATIONS